

Reactivity-Based Fluoride Detection: Evolving Design Principles for Spring-Loaded Turn-On Fluorescent Probes

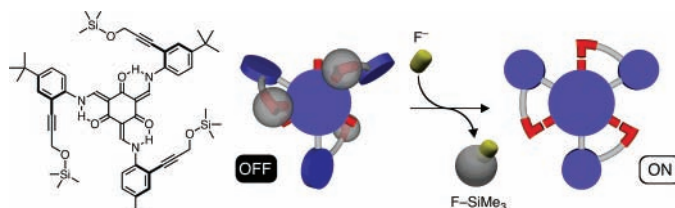
Xuan Jiang, Mario C. Vieweger, John C. Bollinger, Bogdan Dragnea, and Dongwhan Lee*

Department of Chemistry, Indiana University, 800 East Kirkwood Avenue, Bloomington, Indiana 47405

dongwhan@indiana.edu

Received June 18, 2007

ABSTRACT



A covalently triggered fluorescence turn-on detection scheme has been implemented for a tris(*N*-salicylideneamine)-derived dynamic fluorophore. Selective cleavage of strategically placed Si–O bonds by fluoride ion induces spring-loaded conformational transitions that are tightly coupled to fluorescence enhancement.

Conformational switching drives and regulates important signal transduction pathways in biology.¹ Dynamic inter-conversion between the *on*- and *off*-state of signaling proteins is often mediated by reversible covalent modification of key amino acid side residues. Prominent examples include phosphorylation and dephosphorylation of Ser/Tyr residues in many transmembrane proteins, in which covalently introduced local structural distortions are amplified to global conformational changes that initiate a cascade of events.² This ingenious mode of operation displayed by dynamic multi-subunit assemblies continues to inspire the design, synthesis, and application of molecular devices operating in a conceptually parallel manner.³

In this contribution, we describe rational molecular designs to turn on fluorescence signals via covalently triggered conformational switching. Installation of cleavable silyl ether groups to a dynamic fluorophore system enforced structural unfolding and fluorescence quenching. Efficient desilylation by externally added fluoride ion, however, triggered spontaneous structural folding and the recovery of an intense blue emission originating from a planar conjugated tris(*N*-salicylideneaniline) motif.⁴ A general design strategy to exploit the high selectivity inherent to reactivity-based detection schemes constitutes the main topic of this paper.

We have recently shown that structural folding and unfolding motions of the C_3 -symmetric compound **1** (Figure 1) can reversibly modify its emission properties.^{4c} Specifically, loss of structural rigidity upon disruption of the cyclic

(1) *Transduction Channels in Sensory Cells*; Frings, S., Bradley, J., Eds.; Wiley–VCH: Weinheim, 2004.

(2) Krauss, G. *Biochemistry of Signal Transduction and Regulation*, 3rd ed.; Wiley–VCH: Weinheim, 2003.

(3) (a) Balzani, V.; Credi, A.; Raymo, F. M.; Stoddart, J. F. *Angew. Chem., Int. Ed.* **2000**, *39*, 3348–3391. (b) *Molecular Switches*; Feringa, B. L., Ed.; Wiley–VCH: Weinheim, 2001. (c) Balzani, V.; Venturi, M.; Credi, A. *Molecular Devices and Machines: A Journey into the Nanoworld*; Wiley–VCH: Weinheim, 2003. (d) Bonnet, S.; Collin, J.-P.; Koizumi, M.; Mobian, P.; Sauvage, J.-P. *Adv. Mater.* **2006**, *18*, 1239–1250.

(4) (a) Riddle, J. A.; Bollinger, J. C.; Lee, D. *Angew. Chem., Int. Ed.* **2005**, *44*, 6689–6693. (b) Riddle, J. A.; Lathrop, S. P.; Bollinger, J. C.; Lee, D. *J. Am. Chem. Soc.* **2006**, *128*, 10986–10987. (c) Jiang, X.; Bollinger, J. C.; Lee, D. *J. Am. Chem. Soc.* **2006**, *128*, 11732–11733. (d) Lim, Y.-K.; Jiang, X.; Bollinger, J. C.; Lee, D. *J. Mater. Chem.* **2007**, *17*, 1969–1980. (e) Riddle, J. A.; Jiang, X.; Huffman, J.; Lee, D. *Angew. Chem., Int. Ed.* **2007**, *46*, in press.

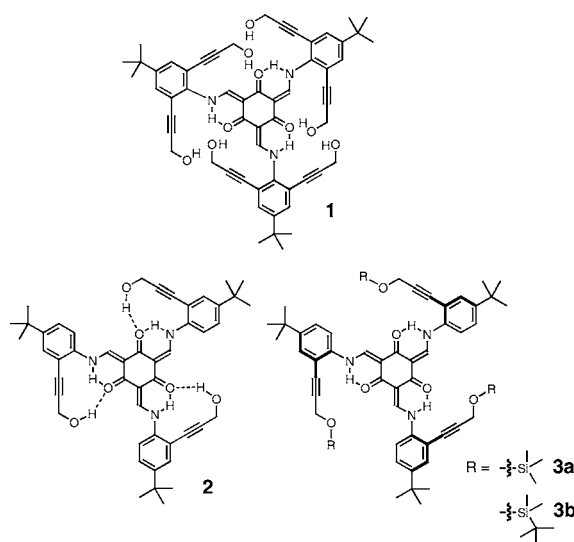
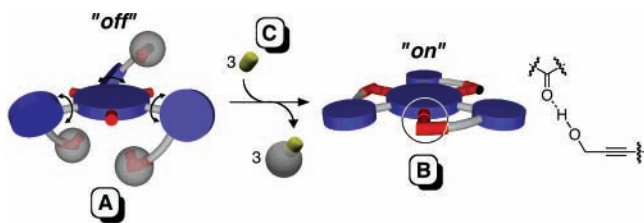


Figure 1. Chemical structures of dynamic fluorophores.

hydrogen-bonding network in **1** facilitated nonradiative decay of its excited states. This was evidenced by fluorescence quenching of **1** by F^- , which engages in competitive $F^- \cdots H-O_{\text{hydroxy}}$ hydrogen bonds and blocks the key anchoring points for its mobile aniline units. Although this process represented an intriguing signal transduction via controllable conformational switching, the *turn-off* mode of operation significantly compromised its practicality as a detection scheme for F^- . In the quest for a structural platform enabling *turn-on* signaling, it was immediately brought to our attention that the molecular mechanism of fluorescence quenching itself could be exploited to our advantage. A conceptual reversal of this structure–property relationship has indeed guided our mechanism-based molecular reengineering as described below.

Scheme 1. Mechanism of Turn-On Detection in which Reaction between **C** and Non-Emissive **A** Furnishes Emissive **B**

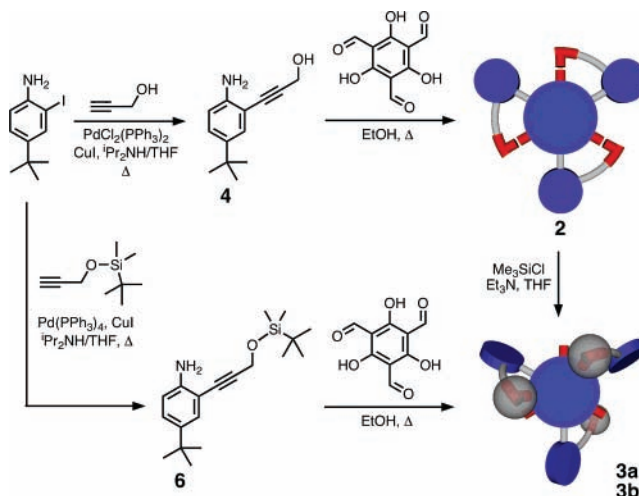


As shown in Scheme 1, our molecular prototype **A** has bulky substituents installed on the “wing-tip” O–H groups of its three mobile components. Steric crowding and the lack of attractive interactions prevent structural folding and furnish torsionally flexible and therefore weakly emissive **A**. A chemical reaction between **A** and **C**, however, can remove these capping groups and expose the O–H groups. Subsequent formation of the key $O_{\text{hydroxy}}-H \cdots O_{\text{carbonyl}}$ hydrogen-

bonding networks drives spontaneous structural folding to **B**, the torsionally rigid nature of which should result in enhanced fluorescence efficiency.

The feasibility of this “spring-loaded” mechanism was tested against new C_3 -symmetric fluorophores **3a–b** (Figure 1). A high-yielding Sonogashira–Hagihara cross-coupling between 2-iodo-4-*tert*-butylaniline and propargyl alcohol afforded **4**, which was reacted with 1,3,5-triformylphloroglucinol in refluxing EtOH to furnish the desired triple Schiff base condensation product **2** in 81% yield (Scheme 2).

Scheme 2. Synthetic Routes to **2**, **3a**, and **3b**



Simple treatment of a THF solution of **2** with $TMSCl/Et_3N$ cleanly afforded **3a** as a yellow solid in 73% yield.^{5,6} On the other hand, an analogue of **3a** having TBDMS groups could be prepared by direct condensation reaction between **6** and 1,3,5-triformylphloroglucinol, which furnished **3b** in essentially quantitative (>99%) yield.

The C_3 -symmetric tris(*N*-salicylideneamine) core structure of **2** was initially suggested by its characteristic $N_{\text{enamine}}-H$ proton doublet resonance at 13.77 ppm, which is coupled ($J = 13.2$ Hz) to the $C_{\text{vinyl}}-H$ doublet at 8.70 ppm.⁴ The proton signal associated with the O–H groups on the peripheral aniline fragments appeared as a triplet ($J = 5.6$ Hz) at 5.36 ppm, which was significantly downfield-shifted compared with that (1.68 ppm) of its model compound 3-phenyl-prop-2-yn-1-ol. This observation strongly implicated their involvement in the hydrogen-bonding interactions with the carbonyl oxygen atoms at the core (Figure 1), which was subsequently confirmed by X-ray crystallography.

The solid-state structure of **2**, shown in Figure 2, revealed an essentially coplanar arrangement of the entire molecule reinforced by three $C=O \cdots H-N$ hydrogen bonds surrounding the six-membered ring at the core. Notably, the wing-

(5) Compound **3a** was obtained as mixture of two stereoisomers of local C_{3h} and C_s symmetry associated with its tris(*N*-salicylideneamine) core.⁴ On the other hand, **3b** was obtained exclusively as the C_{3h} -symmetric isomer. Despite this stereochemical inhomogeneity, similar absorption and emission spectra were obtained for **3a** and **3b**.

(6) See Supporting Information.

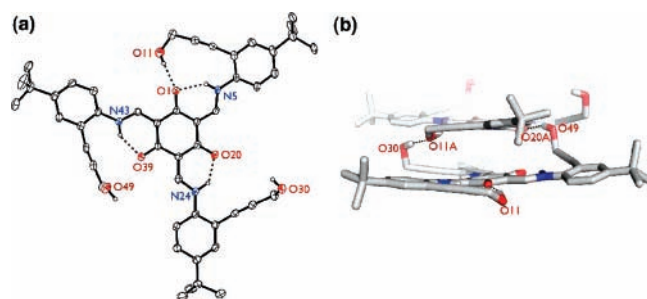


Figure 2. X-ray structure of **2**: (a) ORTEP diagram with thermal ellipsoids at 50% probability; (b) capped-stick representation of a dimeric unit constituting hydrogen-bonded stacks of **2** in the solid state. All the hydrogen atoms, except for those associated with the N–H and O–H groups, have been omitted for clarity. Two of the three tert-butyl groups in **2** are disordered over two positions,⁶ for which only one model is shown. Selected interatomic distances (Å): O11...O1, 2.771; O49...O20A, 2.699; O30...O11A, 2.689; O1...N5, 2.615; O39...N43, 2.594; O20...N24, 2.634.

tip O–H groups of **2** engage in hydrogen-bonding not only in the expected intramolecular fashion (for O11) but also in the rather unanticipated intermolecular fashion (for O30 and O49), which presumably arises from solid-state packing interactions. Specifically, the dangling O–H groups in **2** (Figure 2a) participate in either O–H...O–H (for O30) or O–H...O=C (for O49) hydrogen-bonds with an adjacent molecule of **2** to define interdigitated stacks in the lattice. Under dilute ($\sim 1.0 \mu\text{M}$) conditions used for fluorescence measurements (vide infra), however, the solution population of **2** should be dominated by the intramolecularly hydrogen-bonded structures shown in Figure 1. This was supported by the linear relationship between the concentration and the absorption/emission intensities determined for $[\mathbf{2}] = 0\text{--}1.4 \mu\text{M}$.

In CH_2Cl_2 at 298 K, **2** displays intense ($\epsilon = 93000 \text{ M}^{-1} \text{ cm}^{-1}$) visible absorptions at $\lambda_{\text{max,abs}} = 420$ and 440 nm (Figure S1, Supporting Information). Upon excitation at 340 nm, **2** emits at $\lambda_{\text{max,em}} = 458$ nm with a small Stokes shift (945 cm^{-1}), which reflects the rigid molecular structure. Notably, the fluorescence quantum yield ($= \Phi_{\text{F}}$) of **2** is 9.7(4)%, which is significantly higher than that of **1** (4.2(2)%).^{4c}

Silylation of the key OH groups in **2** no longer supports the rigidifying $\text{O}_{\text{hydroxy}}\text{--H}\cdots\text{O}_{\text{carbonyl}}$ hydrogen-bonding networks. The complete disappearance of the longest wavelength absorption at 440 nm and blue-shift of the transition at 345 nm (Figure S1) presumably reflect structural distortion and decrease in the 2-D conjugation area spanned by **3a**. This covalent modification also results in significant decrease in the emission quantum yield, with Φ_{F} values of 3.4(1) and 4.3(1)% determined for **3a** and **3b**, respectively.

The solution dynamics of **2** and **3a** were further probed by time-correlated single photon fluorescence spectroscopy (Figure S2, Supporting Information).⁶ In CH_2Cl_2 at 293 K, average radiative decay rate constants (k_{r}) of 0.290 and 0.281 ns^{-1} were obtained for **2** and **3a**, respectively, indicating that

silylation of the OH groups in **2** did not fundamentally affect the emissive decay pathways. On the other hand, **2** and **3a** display markedly different nonradiative decay rate constants (k_{nr}) of 2.70 and 8.00 ns^{-1} , respectively. The increased torsional freedom of **3a** (Scheme 1) and the presence of dangling trimethylsilyl groups apparently facilitate nonradiative relaxation of the excited states, thereby effectively decreasing Φ_{F} .^{7–9}

Upon addition of F^- (0.1 mM, $n\text{Bu}_4\text{NF}$), a CH_2Cl_2 solution sample of **3a** ($1.0 \mu\text{M}$) displayed >3-fold enhancement in the fluorescence signal (Figure 3a). The time-dependent

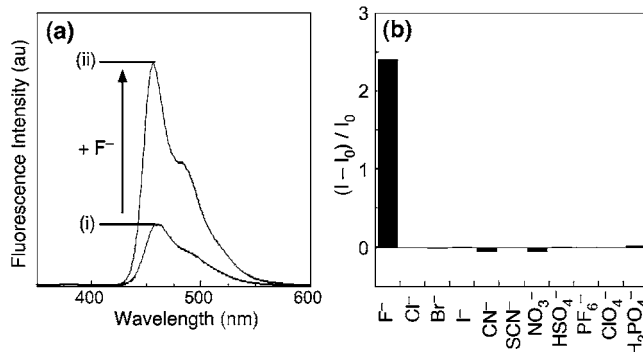


Figure 3. (a) Emission spectra of **3a** ($1.0 \mu\text{M}$) (i) prior to and (ii) after addition of $n\text{Bu}_4\text{NF}$ (0.1 mM) in CH_2Cl_2 with $\lambda_{\text{exc}} = 340 \text{ nm}$. (b) Fluorescence signal response of **3a** ($1.0 \mu\text{M}$) to different anionic species ($50 \mu\text{M}$) added as their tetrabutylammonium salts in CH_2Cl_2 . The response was quantified as $(I - I_0)/I_0$, in which I_0 and I represent fluorescence intensity of **3a** prior to and after addition of the analyte, respectively. Measurements were made after a 20 min period after addition at $T = 25^\circ\text{C}$.

increase in the emission intensity displayed *pseudo* first-order-type kinetics with an increasing overall rate with increasing $[\text{F}^-]$ (Figure S3, Supporting Information), which points toward the participation of both **3a** and F^- in the rate-determining step leading to fluorescence turn-on.¹⁰

Mass spectrometric analysis of the reaction mixture of **3a** + F^- revealed peaks corresponding to a $[\mathbf{2} + \text{Na}]^+$ ion ($m/z = 788.3670$). In addition, the UV–vis spectrum obtained for this reaction mixture was essentially identical to that obtained for **2** (Figures S1 and S4, Supporting Information). These findings fully corroborate the formation of **2** as the desilylation product of **3a**. Under similar conditions, reactions between **3b** and F^- did not result in any noticeable change in the emission signal, which is presumably due to the more robust nature of the $\text{O--SiMe}_2\text{Bu}$ bond relative to the O--SiMe_3 bond against nucleophilic attack by F^- .¹¹

(7) Pyun, C.-H.; Lyle, T. A.; Daub, G. H.; Park, S.-M. *Chem. Phys. Lett.* **1986**, *124*, 48–52.

(8) Turro, N. J. *Modern Molecular Photochemistry*; University Science Books: Sausalito, CA, 1991.

(9) Valeur, B. *Molecular Fluorescence: Principles and Applications*; Wiley-VCH: Weinheim, Germany, 2002.

(10) Detailed kinetic analysis of process, however, was hampered by the multiple O--SiMe_3 groups in **3a** which can react with F^- as well as by the formation of partially desilylated products at the early stage of the reaction that can potentially contribute to the experimentally observed fluorescence enhancement.

The mechanism of fluorescence turn-on in this system is based exclusively on the Si–O bond cleavage reactions of **3a** which can be effected by F[−] under mild conditions to generate **2**. The high-level of selectivity attained by this reactivity-based detection scheme was convincingly demonstrated by the screening of **3a** against 11 different anions. As shown in Figure 3b, only F[−] elicited measurable increase in the fluorescence signal, whereas Cl[−], Br[−], I[−], CN[−], SCN[−], NO₃[−], HSO₄[−], PF₆[−], ClO₄[−], and H₂PO₄[−] had no effect under similar conditions.

The turn-on detection scheme shown in Figure 3 relies critically on the inertness of **2** toward F[−]. Unlike the situation with **1**,^{4c} treatment of an excess (>100 equiv) amount of F[−] did not elicit any noticeable changes in the emission spectra of **2**. Use of the silyl ether derivative of **1** analogous to **3a** would suffer from unreacted F[−] that can interact with the initially generated product **1** to cause eventual diminution of the initial turn-on response.

Increasing concerns regarding environmental protection and national security has fueled research efforts to detect fluoride ion released as the hydrolysis product of toxic organophosphonate agents. Fluorescent probes developed for fluoride ion typically integrate multidentate hydrogen-bonding arrays as receptor units.¹² The compact (ionic radius = 1.15 Å) and basic (pK_a = 3.2) nature of fluoride ion makes it an ideal target of such state-of-the-art “coordination”-based detection scheme.^{13,14} An alternative approach that exploits the intrinsic chemical reactivity of fluoride ion toward Lewis acidic boron or silicon atom is a promising but much less explored avenue. Previous examples include triarylborane-based fluorophores that respond by perturbation of the electronic conjugation as a result of B–F bond formation,^{15,16} luminescent triaryldifluorosilicates obtained by Si–F bond formation of triarylfluorosilanes,¹⁷ or fluoride-triggered Si–O

bond cleavage leading to cyclization of a coumarin precursor,¹⁸ some of which display highly selective turn-on signal response similar to **3a**.^{15a–c,17,18}

In summary, preprogrammed conformational switching¹⁹ of a covalently modifiable fluorophore was exploited for turn-on detection of fluoride ion. The conceptual framework of this spring-loaded mechanism should be generally applicable to other chemical transformations that can restore the structural rigidity and thereby enhance the emission properties of a dynamic fluorogenic platform. Efforts are currently underway in our laboratory to expand the scope of this chemistry.

Acknowledgment. This work was supported by Indiana University, the National Science Foundation (CAREER CHE 0547251), the American Chemical Society Petroleum Research Fund (42791-G3), and the Indiana METACyt Initiative funded through a major grant from the Lilly Endowment, Inc.

Supporting Information Available: Experimental details of the preparation and characterization of synthetic intermediates and X-ray crystallographic data. This material is available free of charge via the Internet at <http://pubs.acs.org>.

OL7014187

(11) Greene, T. W.; Wuts, P. G. M. *Protective Groups in Organic Synthesis*, 3rd ed.; John Wiley & Sons: Hoboken, NJ, 1999.

(12) For recent reviews on anion sensing with luminescent probes, see: (a) Beer, P. D.; Gale, P. A. *Angew. Chem., Int. Ed.* **2001**, *40*, 486–516. (b) Lavigne, J. J.; Anslyn, E. V. *Angew. Chem., Int. Ed.* **2001**, *40*, 3118–3130. (c) Martínez-Máñez, R.; Sancenón, F. *Chem. Rev.* **2003**, *103*, 4419–4476. (d) Gunnlaugsson, T.; Glynn, M.; Tocci, G. M.; Kruger, P. E.; Pfeffer, F. M. *Coord. Chem. Rev.* **2006**, *250*, 3094–3117.

(13) For urea-based luminescent probes for fluoride ion, see: (a) Gunnlaugsson, T.; Davis, A. P.; Glynn, M. *Chem. Commun.* **2001**, 2556–2557. (b) Kim, S. K.; Yoon, J. *Chem. Commun.* **2002**, 770–771. (c) Cho, E. J.; Moon, J. W.; Ko, S. W.; Lee, J. Y.; Kim, S. K.; Yoon, J.; Nam, K. C. *J. Am. Chem. Soc.* **2003**, *125*, 12376–12377. (d) Xu, G.; Tarr, M. A. *Chem. Commun.* **2004**, 1050–1051. (e) Oton, F.; Tarraga, A.; Espinosa, A.; Velasco, M. D.; Molina, P. *J. Org. Chem.* **2006**, *71*, 4590–4598. (f) Zhao, Y.-P.; Zhao, C.-C.; Wu, L.-Z.; Zhang, L.-P.; Tung, C.-H.; Pan, Y.-J. *J. Org. Chem.* **2006**, *71*, 2143–2146.

(14) For calix[4]pyrrole-derived luminescent probes and their analogues for fluoride detection, see: (a) Black, C. B.; Andrioletti, B.; Try, A. C.; Ruiperez, C.; Sessler, J. L. *J. Am. Chem. Soc.* **1999**, *121*, 10438–10439. (b) Miyaji, H.; Anzenbacher, P., Jr.; Sessler, J. L.; Bleasdale, E. R.; Gale, P. A. *Chem. Commun.* **1999**, 1723–1724. (c) Anzenbacher, P., Jr.; Jursikova, K.; Sessler, J. L. *J. Am. Chem. Soc.* **2000**, *122*, 9350–9351. (d) Anzenbacher, P., Jr.; Try, A. C.; Miyaji, H.; Jursikova, K.; Lynch, V. M.; Marquez, M.; Sessler, J. L. *J. Am. Chem. Soc.* **2000**, *122*, 10268–10272. (e) Cho, W.-S.; Sessler, J. L. In *Functional Synthetic Receptors*; Schrader, T., Hamilton, A. D., Eds.; Wiley-VCH: Weinheim, 2005; pp 165–256.

(15) (a) Yamaguchi, S.; Shirasaka, T.; Akiyama, S.; Tamao, K. *J. Am. Chem. Soc.* **2002**, *124*, 8816–8817. (b) Kubo, Y.; Yamamoto, M.; Ikeda, M.; Takeuchi, M.; Shinkai, S.; Yamaguchi, S.; Tamao, K. *Angew. Chem., Int. Ed.* **2003**, *42*, 2036–2040. (c) Liu, X. Y.; Bai, D. R.; Wang, S. *Angew. Chem., Int. Ed.* **2006**, *45*, 5475–5478. (d) Lee, M. H.; Agou, T.; Kobayashi, J.; Kawashima, T.; Gabbai, F. P. *Chem. Commun.* **2007**, 1133–1135.

(16) For other systems relying on B–F bond formation for fluorescence detection, see: (a) Cooper, C. R.; Spencer, N.; James, T. D. *Chem. Commun.* **1998**, 1365–1366. (b) Arimori, S.; Davidson, M. G.; Fyles, T. M.; Hibbert, T. G.; James, T. D.; Kociok-Köhn, G. I. *Chem. Commun.* **2004**, 1640–1641. (c) Xu, S.; Chen, K.; Tian, H. *J. Mater. Chem.* **2005**, *15*, 2676–2680.

(17) Yamaguchi, S.; Akiyama, S.; Tamao, K. *J. Am. Chem. Soc.* **2000**, *122*, 6793–6794.

(18) Kim, T.-H.; Swager, T. M. *Angew. Chem., Int. Ed.* **2003**, *42*, 4803–4806.

(19) For a recent example of hydrogen-bonding mediated conformational control of anion receptors, see: Santacrose, P. V.; Davis, J. T.; Light, M. E.; Gale, P. A.; Iglesias-Sánchez, J. C.; Prados, P.; Quesada, R. *J. Am. Chem. Soc.* **2007**, *129*, 1886–1887.